

Dynamic characteristics of base-isolated shear buildings

T.-C. Pan

Nanyang Technological University, Singapore

ABSTRACT: An analytical investigation on the dynamic characteristics, in the linear elastic range, of shear beam type buildings supported on the laminated rubber bearings is carried out. The superstructure is modeled as a continuum shear beam. The base raft forming part of the base-isolated building is taken as a mass lumped at the lower end of the shear beam, while the effective linear stiffness is assumed for the bearings. In addition to the base-isolated shear beam, close form solutions of two auxiliary shear beams with free-spring and unconstrained end conditions are obtained for comparison. The frequencies of the base-isolated shear beam are found to fall into a range bounded by those of the auxiliary shear beams. The higher modes of the base-isolated beam are practically identical with those of the unconstrained shear beam and therefore orthogonal to the horizontal ground motion. The contribution of higher modes toward the response of superstructure is therefore negligible.

1 INTRODUCTION

Base isolation has become an increasingly accepted technique to decouple a building from the horizontal components of earthquake ground motion. Many ingenious mechanisms have been developed to achieve the decoupling effects, while carrying the vertical load of the building, but only a few practical systems have been implemented in real buildings. Among those implemented, the laminated rubber bearing is perhaps the simplest and most convenient.

It has been shown in previous analyses that seismic response of base-isolated structures can be obtained by modeling the superstructures as rigid blocks supported on isolation systems (Kelly (1990), Pan and Kelly (1983, 1984)). Su et. al. (1989a) carried out a comparative study of various base isolation systems supporting a rigid mass. The rigid block assumption results in a simplified system of single degree of freedom which is suitable for the preliminary design of base-isolated structures.

However, the results obtained based on the rigid block assumption are limited to stiff structures where the influence of flexibility in the superstructure is negligible. Using discrete models, Kelly (1990) and Tsai and Kelly (1989) investigated the effects of superstructure flexibility on the response of a base-isolated structure and its attached equipment. Su et. al. (1989b) carried out numerical investigations for an-

other comparative study of performances of various base isolators for shear beam type structures.

This paper will focus on the analytical investigation on the dynamic characteristics of the base-isolated continuum shear beam model subjected to a horizontal ground motion. In addition to the base-isolated shear beam, two auxiliary shear beam models with free-spring and unconstrained end conditions are also examined. For comparison, the dynamic characteristics of the three types of shear beam are shown in close form expressions. Conclusions are then drawn regarding the shifting of natural frequencies and the contribution of higher modes toward the response of superstructure.

2 SYSTEMS CONSIDERED

One of the simplest but important continuum models for building structures is the shear beam model. In this paper a building structure on a base isolation system is idealized as a uniform shear beam. It is assumed that the base-isolated structure behaves elastically, that the girders are rigid, and that the columns do not deform axially. The mass of the base raft on top of the elastomeric rubber isolation bearings is lumped at the lower end of the uniform shear beam while an elastic spring representing the equivalent effective stiffness of the isolation bearings is attached to the lumped base mass.

The idealized system for the base-isolated shear beam model is shown in Figure 1a. Figures 1b and 1c show the configurations of two auxiliary shear beams which are referred to later in the analysis as the unconstrained shear beam and the free-spring shear beam models, respectively.

The elastic stiffness of a shear beam is represented by GA_s , where G is the modulus of rigidity and A_s is the effective shear area, while the mass per linear length of the shear beam is assumed to be ρA where ρ is the mass density and A is the cross sectional area. However, A_s is related to A through $A_s = \kappa A$ in which κ is the shape factor. The additional spring stiffness and base raft mass due to the base isolation system are represented by k_b and m_b , respectively.

Note that the auxiliary models are actually the limiting cases of the base-isolated shear beam model. The unconstrained shear beam model of Figure 1b can be obtained from the base-isolated shear beam model of Figure 1a by letting $k_b = 0$. The free-spring shear beam model of Figure 1c can be obtained similarly by letting $m_b = 0$.

3 UNDAMPED EQUATIONS OF MOTION

Figure 2a shows the deformation of the base-isolated shear beam subjected to a horizontal ground displacement u_g . The dynamic equilibrium for a segment of the shear beams is shown in Figure 2b. Hence, the equation of motion governing the undamped response of the base-isolated shear beam to the horizontal ground motion is given by

$$\rho A \ddot{Y}(x, t) - GA_s Y''(x, t) = -\rho A \ddot{u}_g(t)$$

where dots and primes indicate differentiation with respect to time t and space x , respectively; $Y(x, t)$ is the displacement response relative to the ground; and $\ddot{u}_g(t)$ is the horizontal ground acceleration motion. Divided by ρA , this equation can be simplified as

$$\ddot{Y} - c^2 Y'' = -\ddot{u}_g(t) \quad (1)$$

in which $c = (GA_s/\rho A)^{1/2} = (\kappa G/\rho)^{1/2}$ is the shear wave velocity propagating through the beam.

Assuming that the height of the shear beam is ℓ , the boundary conditions at the beam ends for $x = \ell$ and $x = 0$, respectively, take the form

$$Y'(\ell, t) = 0 \quad (2)$$

and

$$m_b(\ddot{Y}(0, t) + \ddot{u}_g) + k_b Y(0, t) = GA_s Y'(0, t) \quad (3)$$

in which m_b is the mass of base raft and k_b is the stiffness of base isolators. These equations prescribe the zero slope condition at the free end and the dynamic equilibrium condition of the base mass as shown in Figure 2c.

Let $Y_b(t)$ be the base displacement and $v(x, t)$ be the shear beam displacement relative to the base raft as shown in Figure 2a, that is

$$v(x, t) = Y(x, t) - Y(0, t) = Y(x, t) - Y_b(t).$$

Then, both the equation of motion and the boundary conditions can alternatively be expressed in terms of the relative displacement v

$$\ddot{v} - c^2 v'' = -(\ddot{Y}_b + \ddot{u}_g)$$

The boundary conditions for $v(x, t)$ are

$$v'(\ell, t) = 0, \quad v(0, t) = 0$$

Note that $v'(x, t) = Y'(x, t)$, and the equation governing the motion of the base raft therefore becomes

$$m_b(\ddot{Y}_b + \ddot{u}_g) + k_b Y_b = GA_s v'(0, t) = GA_s Y'_b$$

3.1 Limiting cases

The auxiliary shear beam models as shown in Figures 1b and 1c differ from the base-isolated shear beam model only in the boundary condition at the lower end of the beams. The auxiliary models are actually the limiting cases of the base-isolated shear beam model, and therefore their boundary conditions can be obtained by letting m_b or k_b of equation (3) approach zero separately.

- Unconstrained Shear Beam ($k_b \rightarrow 0$)

$$m_b(\ddot{Y}_b + \ddot{u}_g) = GA_s Y'_b$$

- Free-Spring Shear Beam ($m_b \rightarrow 0$)

$$k_b Y_b = GA_s Y'_b$$

4 ANALYSIS PROCEDURE

4.1 Eigenvalue problem

The eigenvalue problem associated with the equation of motion of equation (1) and the boundary conditions of equations (2) and (3) for the base-isolated shear beam can be obtained from the following homogeneous equation

$$\ddot{Y} - c^2 Y'' = 0 \quad (4)$$

with the homogeneous boundary conditions

$$Y'(\ell, t) = 0 \quad (5)$$

and

$$m_b \ddot{Y}_b + k_b Y_b = GA_s Y'_b \quad (6)$$

Separation of variables is used to analyze the free vibration equation of the system. Let

$$Y(x, t) = \phi(x)q(t)$$

which, when substituted into equation (4), leads to the following two ordinary differential equations:

$$\ddot{q} + \omega^2 q = 0 \quad (7)$$

and

$$\phi'' + \lambda^2 \phi = 0 \quad (8)$$

where

$$\omega^2 = \lambda^2 c^2 = \lambda^2 \kappa G / \rho$$

in which ω is the natural frequency of the base-isolated shear beam and λ is a frequency parameter. Similarly, after substituting and simplification, the homogeneous boundary conditions of equations (5) and (6) take the form

$$\phi'(\ell) = 0 \quad (9)$$

and

$$m_b \lambda^2 c^2 \phi(0) - k_b \phi(0) + GA_s \phi'(0) = 0 \quad (10)$$

The homogeneous boundary value problem represented by equations (8), (9), and (10) constitutes the eigenvalue problem for the base-isolated shear beam model. However, it should be noted that with the presence of eigenvalue in the boundary condition of equation (10), this problem is a special case of the general eigenvalue problem (Meirovitch 1967).

Limiting cases

The eigenvalue problems associated with the auxiliary models differ from that of the base-isolated shear beam model only in the boundary condition at the lower end of the beams. Therefore, the homogeneous boundary conditions of the auxiliary models can be arrived by letting m_b or k_b in equation (10) approach zero separately.

- Unconstrained Shear Beam ($k_b \rightarrow 0$)

$$m_b \lambda^2 c^2 \phi(0) + GA_s \phi'(0) = 0$$

- Free-Spring Shear Beam ($m_b \rightarrow 0$)

$$-k_b \phi(0) + GA_s \phi'(0) = 0$$

4.2 Eigensolution

The solution to the homogeneous equation (8) takes the form

$$\phi(x) = a \sin \lambda x + b \cos \lambda x$$

in which a and b are constants to be determined from the boundary conditions. Substituting this equation into equations (9) and (10), the non-trivial solutions can be obtained from the characteristic equation given by

$$\tan \lambda \ell = -\frac{m_b}{m} \lambda \ell + \frac{1}{\lambda \ell} \frac{k_b}{GA_s / \ell}$$

in which $m = \rho A \ell$ is the total mass of the shear beam above the base raft. The non-trivial solutions result in an infinite sequence of discrete eigenvalues for the base-isolated shear beam model of finite length.

For convenience, the characteristic equation can be rewritten into a simpler form

$$\tan \theta_n = -\beta \theta_n + \frac{\alpha}{\theta_n} \quad (11)$$

where

$$\theta_n = \lambda_n \ell = \frac{\omega_n \ell}{c},$$

$$\alpha = \frac{k_b}{GA_s / \ell}, \quad \text{and} \quad \beta = \frac{m_b}{m}.$$

The dimensionless parameters α and β are the stiffness and mass ratios of the base isolation system to the shear beam, respectively.

If θ_n denotes the n th solution to equation (11), the corresponding n th eigenfunction $\phi_n(x)$ can be expressed by

$$\begin{aligned} \phi_n(x) &= b_n (\tan \theta_n \sin \lambda_n x + \cos \lambda_n x) \\ &= b_n \left[\left(-\beta \theta_n + \frac{\alpha}{\theta_n} \right) \sin \frac{\theta_n x}{\ell} + \cos \frac{\theta_n x}{\ell} \right] \\ &= b_n \eta_n(x) \end{aligned} \quad (12)$$

where the arbitrary scale factor $b_n = \phi_n(0)$ is at the base raft level, and therefore $\eta_n(x)$ represents the relative mode shape of the superstructure with respect to the base raft.

Limiting cases

The characteristic equation of a limiting case can similarly be obtained from the requirement of non-trivial solutions satisfying their corresponding boundary conditions. The characteristic equation and the eigen functions for the two limiting cases are summarized as follows:

- Unconstrained Shear Beam ($k_b \rightarrow 0$)

$$\tan \theta_n = -\beta \theta_n \quad (13)$$

$$\begin{aligned} \phi_n(x) &= b_n (\tan \theta_n \sin \lambda_n x + \cos \lambda_n x) \\ &= b_n \left[(-\beta \theta_n) \sin \frac{\theta_n x}{\ell} + \cos \frac{\theta_n x}{\ell} \right] \\ &= b_n \eta_n(x) \end{aligned} \quad (14)$$

- Free-Spring Shear Beam ($m_b \rightarrow 0$)

$$\tan \theta_n = \frac{\alpha}{\theta_n} \quad (15)$$

$$\begin{aligned} \phi_n(x) &= b_n(\tan \theta_n \sin \lambda_n x + \cos \lambda_n x) \\ &= b_n \left[\left(\frac{\alpha}{\theta_n} \right) \sin \frac{\theta_n x}{\ell} + \cos \frac{\theta_n x}{\ell} \right] \\ &= b_n \eta_n(x) \end{aligned} \quad (16)$$

Graphic solutions of the characteristic equation (11) of the base-isolated shear beam model are depicted on Figure 3 for a special case where the non-dimensional parameters α and β are both taken as 0.1. This value of stiffness and mass ratios may be considered representative for typical base-isolated structures using laminated rubber bearings.

4.3 Remarks on frequencies

In Figure 3, the frequency solutions θ_n of the free-spring shear beam, equation (15), are located at the intersections of the dotted line with the tangent function curves in the upper half plane, while those of the unconstrained shear beam, equation (13), are located at the intersections of the dotted line with the tangent function curves in the lower half plane. The frequency equation (11) of the base-isolated shear beam is the combination of the above two limiting cases. Its graphic solutions can therefore be obtained accordingly by combining the two dotted lines for the limiting cases to form the solid line in Figure 3.

From Figure 3, it is clear that solutions to the frequency equations (13) and (15) are the lower and upper bounds, respectively, for those to equation (11). In other words, the frequencies of the base-isolated shear beam fall between those of the unconstrained and the free-spring shear beams.

Figure 3 also shows that the fundamental natural frequency of the base-isolated shear beam is very close to but slightly lower than the first frequency of the free-spring shear beam. The perturbation on the fundamental frequency is caused by the addition of the base mass and reflected by the $(-\beta\theta_n)$ term. Being in the neighborhood of the coordinate origin, the magnitude of perturbation can be very small when both β and θ_n are small.

Furthermore, Figure 3 shows that the frequencies of higher modes of the base-isolated shear beam are very close to but slightly higher than the non-zero frequencies of the unconstrained shear beam. The perturbation on the higher mode frequencies is caused by the spring stiffness of the isolation system and reflected by the α/θ_n term. Since α is usually small for base-isolated buildings and θ_n grows rapidly, the perturbation on the higher frequencies is very small.

It is also interesting to note that when the mass of base raft approaches infinity, the frequencies of the unconstrained shear beam approach those of a corresponding fixed-base shear beam at $\theta_n = (n - 1/2)\pi$ with $n = 1, 2, \dots, \infty$.

In other words, Figure 3 reveals the basic reason why an isolation system works. With the introduction of base isolation, the fundamental frequency is lowered significantly from the fixed-base frequency of $\theta_1 = \pi/2$, while the second frequency is shifted substantially higher toward the first non-zero frequency of a free-spring beam at around $\theta_2 = \pi$. The property of frequency shifting can be judiciously utilized to avoid the dominant frequencies of the earthquake ground motion for general soil conditions. Using discrete models, Kelly (1990) revealed similar properties of base-isolated structures.

4.4 Orthogonal conditions

The linear second order differential operators of the special eigenvalue problem for the various shear beam models used in this study can be shown to be positive and self-adjoint. It can further be shown that the operators of the free-spring and the base-isolated shear beam models are positive definite.

Arising from the positive definite eigenvalue problem for the base-isolated shear beam, the orthogonal conditions with respect to mass and stiffness, respectively, for the eigenfunctions corresponding to the distinct eigenvalues take the form

$$\rho A \int_0^{\ell} \phi_i(x) \phi_j(x) dx + m_b \phi_i(0) \phi_j(0) = 0, \quad i \neq j$$

$$GA_s \int_0^{\ell} \phi_i'(x) \phi_j'(x) dx + k_b \phi_i(0) \phi_j(0) = 0, \quad i \neq j$$

In addition, these orthogonal eigenfunctions can be normalized with respect to mass as shown in the following:

$$\rho A \int_0^{\ell} \phi_i^2(x) dx + m_b \phi_i^2(0) = 1.0$$

This process results in a set of orthonormal eigenfunctions with which the Expansion Theorem can be applied to obtain the response of the base-isolated shear beam $Y(x, t)$ by modal analysis.

Limiting cases

For the auxiliary shear beam models, the orthonormal eigenfunctions with respect to mass and stiffness derived from the base-isolated shear beam are summarized as follows:

- Unconstrained Shear Beam ($k_b \rightarrow 0$)

$$\rho A \int_0^l \phi_i(x) \phi_j(x) dx + m_b \phi_i(0) \phi_j(0) = 0, \quad i \neq j$$

$$GA_s \int_0^l \phi_i'(x) \phi_j'(x) dx = 0, \quad i \neq j$$

$$\rho A \int_0^l \phi_i^2(x) dx + m_b \phi_i^2(0) = 1.0$$

- Free-Spring Shear Beam ($m_b \rightarrow 0$)

$$\rho A \int_0^l \phi_i(x) \phi_j(x) dx = 0, \quad i \neq j$$

$$GA_s \int_0^l \phi_i'(x) \phi_j'(x) dx + k_b \phi_i(0) \phi_j(0) = 0, \quad i \neq j$$

$$\rho A \int_0^l \phi_i^2(x) dx = 1.0$$

4.5 Remarks on mode shapes

The mode shapes of the three types of shear beams can be evaluated from equations (12), (14), and (16). For a typical value of $\alpha = 0.1$, equation (12) approaches rapidly equation (14), i.e. as θ_n grows

$$-\beta \theta_n + \frac{\alpha}{\theta_n} \rightarrow -\beta \theta_n$$

In fact, from the second mode upwards, the higher modes of the base-isolated shear beam are practically identical with those of non-zero frequency for the unconstrained shear beam.

It is important to note that the higher modes of the unconstrained shear beam are orthogonal to its first mode that is a rigid body mode representing the horizontal ground motion. Consequently, the higher modes of the base-isolated shear beams do not absorb energy resulting from the horizontal ground motion; instead, they deflect energy through the property of orthogonality. Using a discrete model, Kelly (1990) revealed similar property for base-isolated structures. Fan and Ahmadi (1990), Tsai and Kelly (1989), and Su et. al. (1989) observed this property in their numerical results showing the remarkably low level of higher mode acceleration transmission to buildings on laminated rubber bearings.

6 CONCLUSIONS

The exact analytical solutions are obtained for the natural frequencies and mode shapes of three types of shear beam models — base-isolated, unconstrained, and free-spring shear beams — as shown in equations

(11-16). The solution process takes into account fully the influence of flexibility in the superstructures.

For $\alpha = 0.1$ and $\beta = 0.1$, typical values for base-isolated buildings on laminated rubber bearings, graphical results are obtained. The results show that the frequencies of the base-isolated shear beam fall into a range, to which the frequencies of the free-spring shear beam form the upper bound while those of the unconstrained shear beam form the lower bound. They also indicate that the first base-isolated frequency is very close to that of the free-spring shear beam, and that the higher frequencies of the base-isolated shear beam are practically identical with those of the free-spring shear beam.

It is also shown that the mode shapes associated with the higher frequencies of base-isolated shear beam approach rapidly those of the unconstrained shear beam, which are orthogonal to the rigid body mode representing the horizontal ground motion. Therefore, it can be concluded that when laminated rubber isolators are used, the contribution of higher modes to the response of superstructure is insignificant, and that such isolated structures in turn provide effective protection to the secondary systems which are usually of high frequency.

REFERENCES

- Fan, F.-G. & Ahmadi, G. 1990. Floor response spectra for base-isolated multi-storey structures. *Earthquake Engineering & Structural Dynamics*, 19: 377-388.
- Kelly, J.M. 1990. Base isolation: Linear theory and design. *Earthquake Spectra*, Vol. 6, No. 2, 223-244.
- Meirovitch, L. 1967. *Analytical methods in vibration*. Macmillan, New York. 138-141.
- Pan, T.-C. & Kelly, J.M. 1983. Seismic response of torsionally coupled base-isolated structures. *Earthquake Engineering & Structural Dynamics*, 11: 749-770.
- Pan, T.-C. & Kelly, J.M. 1984. Seismic response of base-isolated structures with vertical-rocking coupling. *Earthquake Engineering & Structural Dynamics*, 12: 681-702.
- Su, L., Ahmadi, G. & Tadjbakhsh, I.G. 1989a. A comparative study of performance of various base isolation systems, part I: Shear beam structures. *Earthquake Engineering & Structural Dynamics*, 18: 11-32.

Su, L., Ahmadi, G. & Tadjbakhsh, I.G. 1989b. Comparative study of base isolation systems. *J. of Engineering Mechanics, ASCE*, 115: 1976-1992.

Tsai, H.-C. & Kelly, J.M. 1989. Seismic response of the superstructure and attached equipment in a base-isolated building. *Earthquake Engineering & Structural Dynamics*, 18: 551-564.

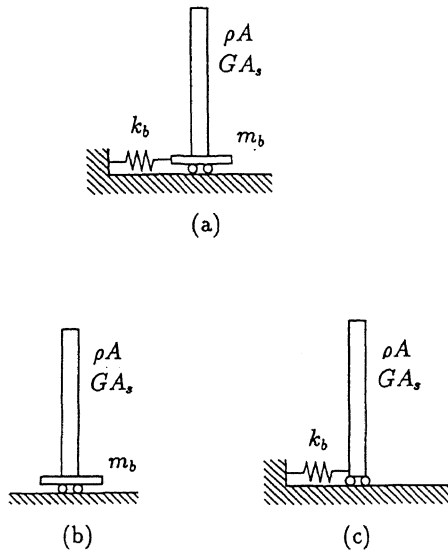


Figure 1. Shear beam models: (a) Base-isolated shear beam, (b) Unconstrained shear beam, and (c) Free-spring shear beam.

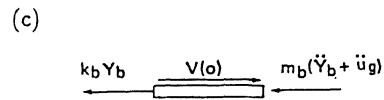
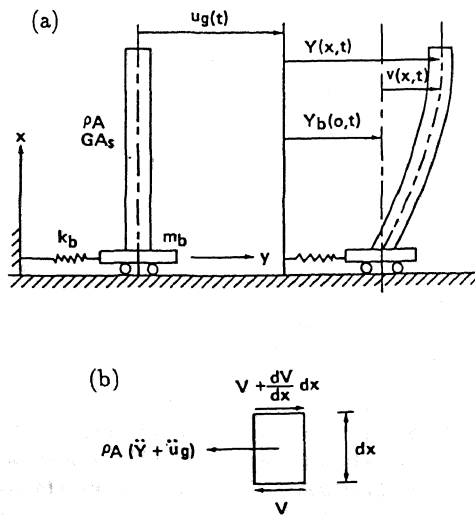


Figure 2. Response of shear beam to ground motion: (a) Deformation, (b) Equilibrium of a segment, and (c) Base raft equilibrium.

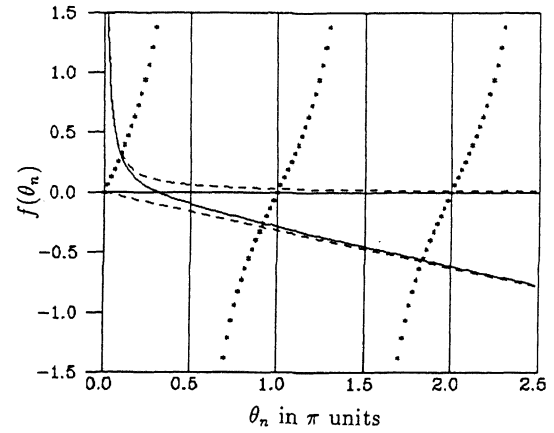


Figure 3. Frequency solutions of the shear beam models ($\alpha = \beta = 0.1$).